Universität Potsdam

Carsten Dosche, Wulfhard Mickler,
Hans-Gerd Löhmannsröben, Nicolas Agenet,
K. P. C. Vollhardt

Photoinduced electron transfer in [N]phenylenes

accepted for publication in:
Journal of Photochemistry and Phtobiology A: Chemistry
ISSN: 1010-6030
DOI: 10.1016/j.jphotochem.2006.12.038

Postprint published at the institutional repository of Potsdam University:
In: Postprints der Universität Potsdam :
Mathematisch-Naturwissenschaftliche Reihe ; 23
http://opus.kobv.de/ubp/volltexte/2007/1246/
http://nbn-resolving.de/urn:nbn:de:kobv:517-opus-12463

Postprints der Universität Potsdam
Mathematisch-Naturwissenschaftliche Reihe ; 23

Photoinduced electron transfer in [N]phenylenes

C. Dosche[a], W. Mickler[a], H.-G. Löhmannsröben[a*], N. Agenet[b] and K. P. C. Vollhardt[b]

[a] *Institute of Chemistry, University of Potsdam, Karl-Liebknecht-Str. 24–25, 14476 Golm, Germany*

[b] *Center for New Directions in Organic Synthesis, Department of Chemistry, University of California at Berkeley and the Chemical Sciences Division, Lawrence Berkeley National Laboratory, Berkeley, California, 94720-1460, USA*

Abstract

First studies of electron transfer in [N]phenylenes were performed in bimolecular quenching reactions of angular [3]- and triangular [4]phenylene with various electron acceptors. The relation between the quenching rate constants k_q and the free energy change of the electron transfer (ΔG^0_{CS}) could be described by the Rehm-Weller equation. From the experimental results, a reorganization energy λ of 0.7 eV was derived.

Intramolecular electron transfer reactions were studied in an [N]phenylene bichomophore and a corresponding reference compound. Fluorescence lifetime and quantum yield of the bichromophor display a characteristic dependence on the solvent polarity, whereas the corresponding values of the reference compound remain constant. From the results, a nearly isoenergonic ΔG^0_{CS} can be determined. As the triplet quantum yield is nearly independent of the polarity, charge recombination leads to the population of the triplet state.

Keywords: [N]phenylenes, photoinduced electron transfer; [N]phenylene dyads

1. Introduction

The [N]Phenylenes represent a completely new class of polycyclic hydrocarbons (PAH), consisting of alternating six- and four-membered rings. As this unusual combination of aromatic and antiaromatic moieties causes outstanding molecular properties, the [N]phenylenes have been object of several synthetic and analytical studies [1]. Also, photophysical studies concerning the geometric effects of electronic excitation on [N]phenylene molecules have been published in the last years [2-4]. The most remarkbale photophysical feature of [N]phenylenes is the striking effect of the annelation geometry on the

internal conversion (IC) in excited linear and angular [N]phenylenes. In contrast to classical PAH, which exhibit usually fluorescence lifetimes (τ_F) of a few ns under ambient conditions, τ_F of the angular members of the [N]phenylenes is in the range of 20–80 ns. These increased values are caused mainly by diminished fluorescence and IC (rate constants k_F and k_{IC}). The low k_F values are due to the forbidden or weakly allowed nature of the S_0–S_1 transitions [2, 3]. In comparison to classical aromatic hydrocarbons, IC of angular [N]phenylenes is remarkably slower [2, 4, 5]. The low k_{IC} values reflect the small extent of geometric distortion between electronic ground and excited states. The observed deviation from a simple energy gap law-type behaviour is caused by the fact that in angular [N]phenylenes only the terminal benzene rings are involved in S_0–S_1 vibronic coupling [2, 4]. These findings are supported by the extraordinarily small Stokes shifts of angular [N]phenylenes, demonstrating the similarity of the structures of ground and excited states for angular [N]phenylenes. In contrast to the angular [N]phenylenes, linear [N]phenylenes are non-fluorescent, or display very short-lived fluorescence (τ_F in the ps-time domain) with very low fluorescence quantum yields (Φ_F) [2]. This is caused by ultrafast IC with rates k_{IC} exceeding 10^9 s^{-1}, due to major geometric distortions between S_0 and S_1 state.

Although the general synthetic procedure introduced by K. C. P. Vollhardt is also suitable for the synthesis of substituted [N]phenylenes [1], photophysical studies have concentrated on unsubstituted [N]phenylenes up to now [2-4]. Recently, the synthesis and first photophysical studies of a donor-acceptor type [N]phenylene dyad have been reported [6]. The authors suggest the combination of a linear [N]phenylene donor with a fullerene acceptor for the use in photovoltaic solar cells, according to photovoltaic fullerene dyads described in the literature [7-10]. However, this seems not promising because k_{IC} of the [N]phenylene chromophor is very high as is evident from the reported lack of fluorescence [6]. Thus, any energy or electron transfer process would have to be very fast in order to compete with IC. Therefore, linear [N]phenylenes are hardly very suitable for functional dyads. On the other hand, the extraordinarily slow IC in angular [N]phenylenes turns these compounds into highly attractive substrates for the study of electron transfer reactions.

In order to elucidate the basic electron transfer properties of angular [N]phenylenes, the bimolecular quenching reactions of angular [3]- (**1**) and triangular [4]phenylene (**2**) (Fig. 1) with various electron acceptors were studied by time-resolved fluorescence spectroscopy. In an extension to the investigation of intramolecular electron transfer reactions, the dyad (**4**) and the corresponding reference substance (**3**) were included.

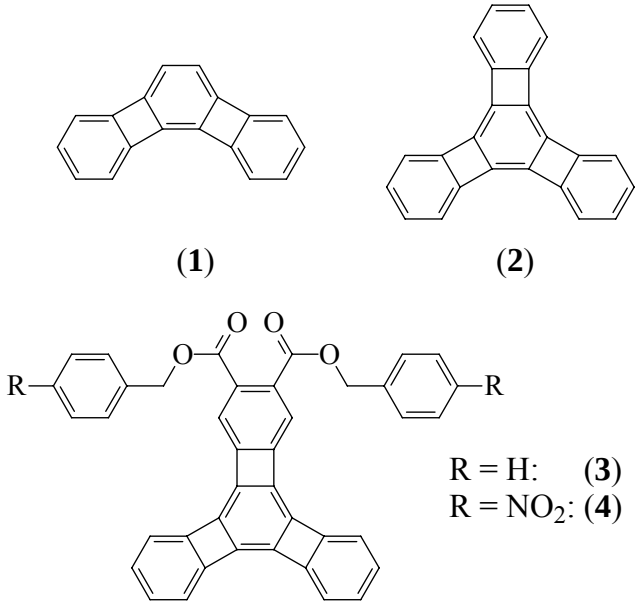

Fig. 1: Structures of the [N]phenylenes

2. Experimental section

Phenylenes (**1**) and (**2**) were synthesized and characterized according to the methods described in the literature [11, 12]. For the synthesis of (**3**) and (**4**), an alkyne coupling protocol modified from that published was employed [13]. For detailed procedures, see synthetic section. Quenchers and reference dyes were purchased at analytical grade (Aldrich, Taufenkirchen, Germany) and used without further purification.

Sample solutions were prepared in HPLC grade solvents. [N]Phenylene concentrations were $5x10^{-5}$ mol/L for fluorescence and 10^{-4} mol/L for transient absorption measurements. Quenching constants k_q were determined by Stern-Volmer analysis using quencher concentrations from $2.5x10^{-3}$ mol/L to $5x10^{-2}$ mol/L.

If not noted otherwise, the measurements are performed at room temperature in 10x10 mm quartz cells (Hellma, Müllheim, Germany). The samples were deoxygenated by flushing with argon for 10 min and sealed with a septum.

For fluorescence measurements at low temperatures, the samples were prepared in a 5x5 mm monolithic quartz cell, flushed for 15 min with argon, and then cooled to 80–280 K with an Optistate DN1704 cryostat (Oxford Instruments, Wiesbaden, Germany) equipped with an external controller (ITC4; Oxford Instruments).

Absorption spectra were recorded with a Cary 500 UV-VIS-NIR spectrophotometer (Varian Inc., Palo Alto, CA, USA). Stationary fluorescence spectra were obtained with a Fluoromax 3 fluorimeter (Jobin Yvon, Edison, NJ, USA). Fluorescence quantum yields in cyclohexane were determined relative to perylene (Φ_F = 1) as reference [14]. Fluorescence and triplet

quantum yields (see below) in other solvents were measured using the solution of the corresponding [N]phenylene in cyclohexane as reference.

Lifetime measurements were performed with a FLS920 fluorimeter (Edinburgh Instruments, Livingston, UK). A frequency-doubled titanium sapphire laser system (Tsunami 3960; Spectra Physics, Mountain View, USA) set at 392 nm was used as the excitation light source. The original repetition rate of 80.2 MHz was reduced to 500 kHz with a pulse picker (Pulse Select; APE, Berlin, Germany). Fluorescence emission was detected with a multichannel plate (ELDY EM1-132/300, Europhoton, Berlin, Germany), providing a time response of ~100 ps.

Transient absorption spectra were recorded using the usual setup consisting of photomultiplier, monochromator and digital storage oscilloscope. The samples were excited with 600 μJ pulses at 355 nm generated by a Nd-YAG-laser (5021 DNS/DPS, B. M. Industries, Evry, France) set at a repetition rate of 5 Hz. Triplet extinction coefficients were determined using rubrene as reference (ε_T (480 nm) ~ 32.000 $M^{-1}cm^{-1}$) [15]. Triplet quantum yields were measured relatively to tetracene [14].

The redox potentials of the compounds (**1**) - (**3**) were determined at a glassy carbon electrode (A = 2.27 mm^2) with an electrochemical analyser BAS 100B (Bioanalytical Systems Inc., West Lafayette, IN, USA). A non-aqueous Ag/Ag^+ electrode was used as reference electrode and a platinum wire as auxiliary electrode. The measurements were performed in a tetrabutylammonium perchlorate solution (0.1 mol/L in acetonitrile) using ferrocene ($\Delta E_{1/2}$ = 85 mV) as internal standard.

The solvent polarity was measured using an ELC-131D meter (Schmidt Scientific, Taipei, Taiwan) connected to a 17.2 pF ring capacitator.

3. Results and Discussion

3.1 Intermolecular electron transfer

Intermolecular electron transfer reactions between an electronically excited fluorophore $^1F^*$ and a quencher Q can be described by the model displayed in Scheme 1 [16].

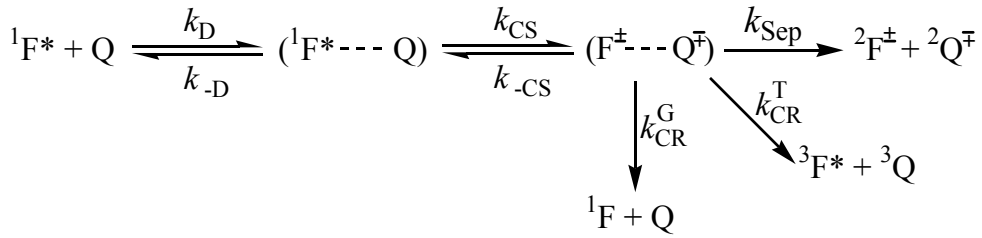

Scheme 1

This model, which was later refined by Farid and Gould (see ref. 17 and references therein), implies the following processes: diffusion controlled formation (rate constant k_D) and dissociation (k_{-D}) of a collision complex (^{1}F*- - -Q) followed by forward and backward charge separation (CS) reactions (k_{CS}, k_{-CS}) yielding the charge transfer complex ($F^{\pm}$- - -$Q^{\pm}$). The latter can dissociate into the free ions $^2F^{\pm}$ and $^2Q^{\pm}$ (k_{Sep}), or undergo charge recombination (CR) reactions producing ground state (^{1}F) or triplet state (^{3}F*) fluorophore molecules (k_{CR}^G, k_{CR}^T). Under steady-state conditions the experimental quenching constant k_q, as determined by Stern-Volmer analysis, can be expressed as a function of the standard free energy change of charge separation (ΔG_{CS}^0) and the corresponding free energy change of activation ($\Delta G_{CS}^{\#}$) [16]:

$$k_q = \frac{k_D}{1 + \frac{k_{-D}}{k_{CS}^0} \cdot e^{\Delta G_{CS}^{\#}/RT} + \frac{k_{-D}}{k_S} \cdot e^{\Delta G_{CS}^0/RT}} \qquad \text{Equ. 1}$$

with $k_S = k_{Sep} + k_{CR}^G + k_{CR}^T$ and $k_{CS}^0 = k_{CS} \cdot \exp(\Delta G_{CS}^{\#}/RT)$.

In an empirical approach, $\Delta G_{CS}^{\#}$ is directly connected to ΔG_{CS}^0 and λ [16,18]:

$$\Delta G_{CS}^{\#} = \frac{\Delta G_{CS}^0}{2} + \left(\left(\frac{\Delta G_{CS}^0}{2} \right)^2 + \left(\frac{\lambda}{4} \right)^2 \right)^{1/2} \qquad \text{Equ. 2}$$

For the determination of λ, the dependence of k_q on ΔG_{CS}^0 has to be evaluated in a so-called Rehm-Weller plot. ΔG_{CS}^0 can be calculated from electrochemical data using the redox potentials of the reaction partners. According to the Weller equation (Equ. 3), ΔG_{CS}^0 of a photoinduced electron transfer is a function of the donor and acceptor redox potentials E_{ox}(D) and E_{red}(A), the excitation energy E_{ex} and the solvent dependent Coulomb term C [19].

$$\Delta G_{CS}^0 = E_{ox}(D) - E_{red}(A) - E_{ex} + C \qquad \text{Equ. 3}$$

The Coulomb term C is relatively small for polar solvents like acetonitrile (ACN) and is therefore often neglected. However, in nonpolar solvents, C as well as the redox potentials change and Equ. 4 can be used for the calculation of ΔG^0_{CS} in less polar solvents [19, 20].

$$\Delta G^0_{CS} = (E_{ox}(D) - E_{red}(A))_{ACN} - E_{ex} + \frac{e^2}{4\pi\varepsilon_0\varepsilon} \cdot \left(\frac{1}{R^{\pm}} - \frac{1}{R_{DA}} \right) - \frac{e^2}{4\pi\varepsilon_0\varepsilon_{ACN}R^{\pm}} \qquad \text{Equ. 4}$$

Here, ε is the solvent polarity, R_{DA} an average donor-acceptor distance and $R^{\pm}$ an average ion radius (obtained under the simplifying assumption that $^2F^{\pm}$ and $^2Q^{\pm}$ can be regarded as identical spheres). Essentially, Equ. 4 allows the recalculation of ΔG^0_{CS} for solvents of different polarities with respect to corresponding data in acetonitrile (denoted by the subscript ACN).

For the experimental determination of λ in [N]phenylene systems, two different approaches were employed. First, ΔG^0_{CS} was varied by using different electron acceptors, which has the inherent disadvantage that λ might also change slightly. Therefore, in a second approach, ΔG^0_{CS} in the (**2**)/nitrotoluene system was varied through a change of the solvent polarity.

In order to estimate ΔG^0_{CS} for the electron transfer reactions between [N]phenylenes (**1**) and (**2**) and selected electron acceptors in acetonitrile, the redox potentials of (**1**) and (**2**) were determined via cyclovoltammetry in acetonitrile. Both compounds exhibit reversible one-electron reduction waves at –2.27 V (**1**) and –2.15 V (**2**), respectively. The peak to peak distance is 120 mV at a scan rate of 100 mV and depends on the scan rate. This points to a hindered electron transfer at the electrode surfaces. At a scan rate of 100 mV/s, both substances show irreversible oxidation at +940 mV and +1020 mV, respectively. However, at higher scan rates (up to 12.8 V/s), the oxidation of (**1**) becomes reversible. This is an indication that in the μs-time domain, in which charge separation and recombination will occur most likely, the oxidation of the [N]phenylene fluorophor is reversible. The redox potentials ($E_{1/2}$) of the electron acceptors used for intermolecular electron transfer reactions and ΔG^0_{CS} calculated for (**1**) and (**2**) are summarized in Table 1.

Tab. 1: Redox potentials vs. SCE of electron acceptors and resulting ΔG^0_{CS} as derived from Weller's equation (*a*: Ref. 24, *b*: Ref. 18, *c*: Ref. 14, *d*: Ref. 25).

Electron acceptor	E_{red} / V	ΔG^0_{CS} (**1**) / eV	ΔG^0_{CS} (**2**) / eV
1,4-Dinitrobenzene	–0.68[a]	–1.27	–1.13
1,2-Dinitrobenzene	–0.79[a]	–1.16	–1.02
1,3-Dinitrobenzene	–0.89[a]	–1.06	–0.92
4-Nitrotoluene	–1.42[b]	–0.53	–0.39
1,4-Dibromobenzene	–1.76[c]	–0.19	–0.05
9-Bromophenanthrene	–2.03[a]	0.08	0.22
Pyrene	–2.09[c]	0.14	0.28
1-Bromonaphthalene	–2.17[d]	0.22	0.36
Chrysene	–2.25[c]	0.30	0.44
Bromobenzene	–2.32[d]	0.37	0.51
Naphthalene	–2.39[b]	0.44	0.58

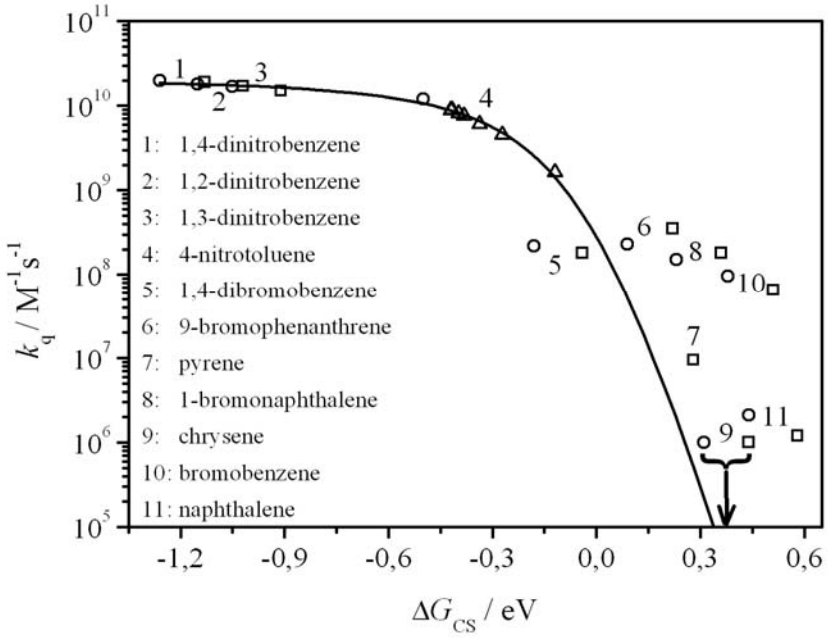

Fig. 2: Rehm-Weller plot for the bimolecular quenching reactions of (**1**) (squares) and (**2**) (circles) with electron acceptors in acetonitrile at 298 K. The values for k_q of the solvent dependent quenching reactions between (**2**) and 4-nitrotoluene are given as triangles. k_q of chrysene is below 10^5 $M^{-1}s^{-1}$. The solid line represents the model function obtained from Equ. 1.

The Rehm-Weller plot for the bimolecular quenching reactions in acetonitrile is displayed in Fig. 2. The solid line represents a fit of the model function (Equ. 1) to the experimental results, with $\Delta G_{CS}^{\#}$ being substituted by Equ. 2 and λ as free parameter. With respect to the other parameters, $k_D = 3\times10^{10}$ $M^{-1}s^{-1}$ and 0.25 for k_{-D}/k_{CS}^{0} and k_{-D}/k_S (as originally introduced by Rehm and Weller) were employed [16]. From this fit, $\lambda = (0.7 \pm 0.1)$ eV was determined. The deviation of 9-bromopenanthrene, 1-bromonaphthalene and bromobenzene from the fit is caused by an increase of the intersystem crossing efficiency due to the heavy atom effect.

For measurements on the (**2**)/nitrotoluene system, ΔG_{CS}^{0} was altered by using ethyl acetate/acetonitrile mixtures of different polarities from ε = 6 (ethyl acetate) to ε = 37.5 (acetonitrile). The results are also given in Fig. 2. For the average donor-acceptor distance R_{DA}, a value of 6 Å for $\Delta G_{CS}^{0} \approx -0.8$ eV was used [21], and an average ion radius $R^{\pm} = 4$ Å was assumed. Again, for $\lambda = 0.7$ eV, the model function Equ. 1 with the parameters evaluated for the results obtained in acetonitrile, fits the experimental results (cf. Fig. 2). Thus, despite rough approximation concerning R_{DA} and $R^{\pm}$, the determination of ΔG_{CS}^{0} in nonpolar solvents is sufficient for the evaluation of λ.

3.2 Intramolecular electron transfer

To study intramolecular electron transfer reactions involving [N]phenylene groups, the bichromophor (**4**), which resembles a bridged intramolecular version of the (**2**)/nitrotoluene system, and the corresponding reference compound (**3**) were synthesized. Fluorescence emission and excitation spectra of (**3**) and (**4**) and the absorption spectrum of (**3**) are displayed in Fig. 3. Clearly, the spectral behaviour of the [N]phenylene fluorophore is not influenced noticeably by substitution of the acceptor part of the molecule. However, in comparison to the unsubstituted triangular [4]phenylene (**2**), attachment of the carboxy groups to the chromophor changes the electrochemical and photophysical properties [2]. The 0–0 transition of the bichromophors is red-shifted by 14 nm, from 438 nm to 452 nm. The electron withdrawing effect of the carboxyl groups shifts the oxidation as well as the reduction potential of the [N]phenylene moiety to more positive values. By cyclovoltammetry, the reduction potential of (**3**) is found to be at -1.7 ± 0.1 V and the oxidation potential at 1.2 ± 0.1 V. If ΔG_{CS}^{0} for electron transfer in (**4**) is calculated by using Equ. 3 and the reduction potential of 4-nitrotoluene (Tab. 1), the shift of E_{ox}(D) and E_{ex} results in $\Delta G_{CS}^{0} \approx$ -0.1 eV in acetonitrile. As Equ. 3 is only an approximation (e.g. in respect of neglecting the Coulomb

term *C*), ΔG^0_{CS} for (**4**) can be expected to be around 0 eV. Given the experimental uncertainties, the CS reaction can thus considered to be almost isoenergonic.

The S_0–S_1 transition, which is symmetrically forbidden for (**2**) is allowed in the case of (**3**) and (**4**) because the symmetry of the chromophor is reduced by the carboxy groups. This also causes a decreased fluorescence lifetime for (**3**) of 18 ns (81 for (**2**)). The fluorescence (Φ_F) and intersystem crossing (Φ_{ISC}) quantum yields of (**3**) are 0.16 and 0.40, respectively. From these values, the rate constants for fluorescence ($k_F = 9\times10^6$ s^{-1}), intersystem crossing ($k_{ISC} = 2.2\times10^7$ s^{-1}) and internal conversion ($k_{IC} = 2.4\times10^7$ s^{-1}) can be calculated. As for non substituted [N]phenylenes, the solvent polarity has no effect on the τ_F, Φ_F and Φ_{ISC} values of (**3**). Therefore, (**3**) is a suitable reference for studying electron transfer reactions of (**4**). In nonpolar solvents, (**4**) exhibits nearly the same τ_F, Φ_F and Φ_{ISC} values as (**3**). It follows that there are no additional deactivation paths for (**4**) in nonpolar solvents. In contrast to reference compound (**3**), in polar solvents, τ_F and Φ_F of (**4**) decrease dramatically (Fig. 4), whereas k_F, as calculated from τ_F and Φ_F, remains constant. Despite the change in τ_F, the decay of fluorescence intensity follows first order kinetics in all solvents.

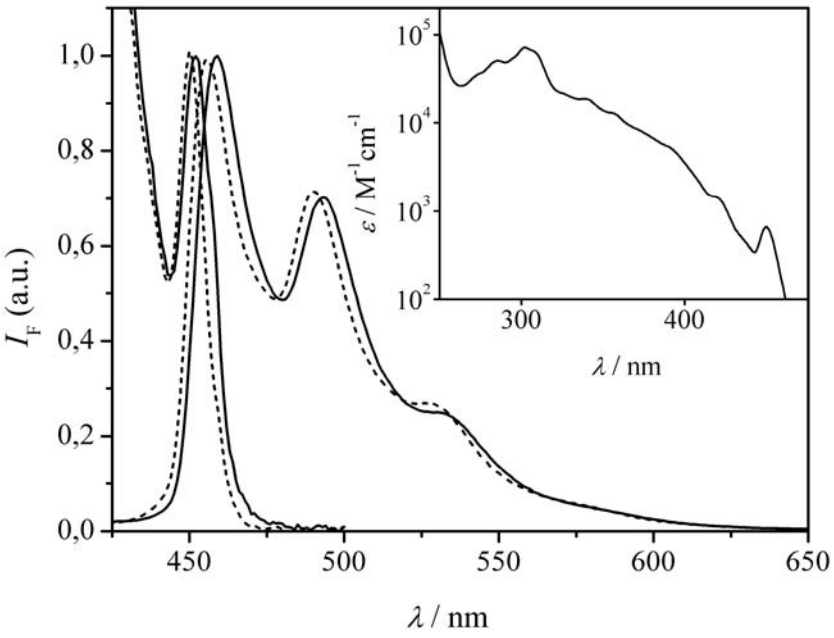

Fig. 3: Excitation (λ_{em} = 500 nm) and fluorescence spectra (λ_{ex} = 400 nm) of (**3**) (dashed) and (**4**) (solid) in ethyl acetate at 298 K. Inset: Absorption spectrum of (**3**) in ethyl acetate.

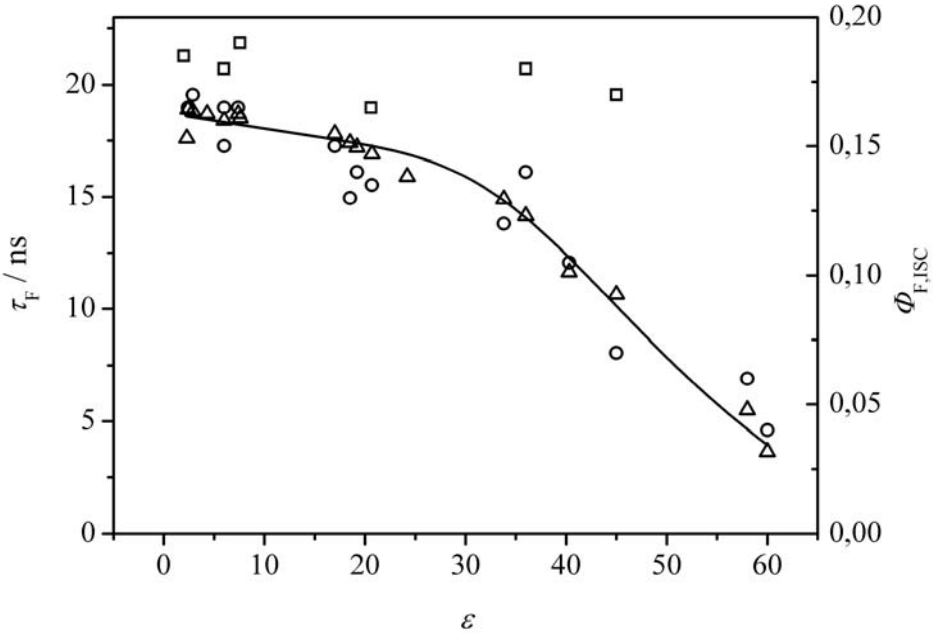

Fig. 4: Solvent effect on fluorescence lifetime (τ_F, triangles), fluorescence quantum yield (Φ_F, circles) and intersystem crossing quantum yields ($\Phi_{ISC}/2$, squares) of (**4**) at 298 K. The solid line represents a fit of Equ. 6 to the experimental data for $\tau_F(\varepsilon)$.

For the results displayed in Fig. 4 a wide variety of solvents and solvent mixtures was used, from nonpolar (cyclohexane; $\varepsilon = 2.1$) to very polar (dimethylformamide/water 1:1; $\varepsilon \approx 60$). It is important to note that different types of solvents, e.g., alkanes, ethers, ketones and nitriles, were used for these experiments. Thus, the observed dependence of τ_F and Φ_F is caused exclusively by the solvent polarity and not by any other solvent properties. Interestingly, Φ_{ISC} is seemingly not influenced by the solvents within experimental error, although is Φ_{ISC} not accessible for $\varepsilon \sim 60$ due to insufficient solubility. (cf. Fig. 4).

In order to explain these observations, Scheme 2 is employed [22], which describes intramolecular in analogy to the intermolecular deactivation (cf. Scheme 1).

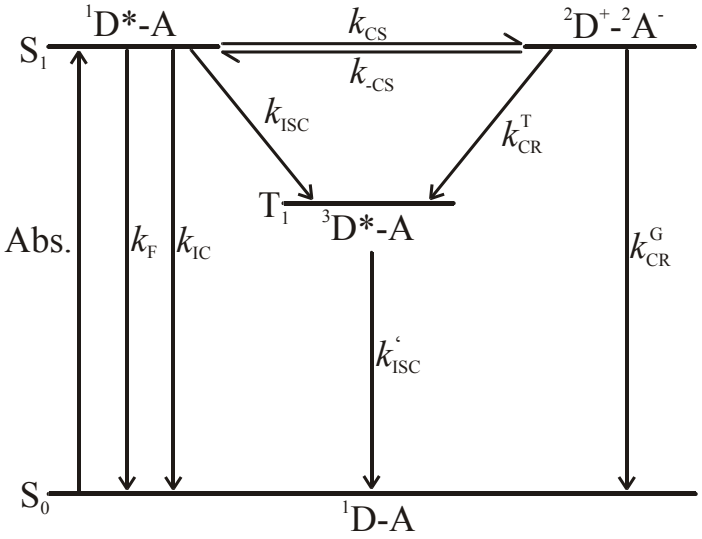

Scheme 2

In this model, an equilibrium between the locally excited bichromophor ^{1}D*–A and the intramolecular charge transfer complex ^{2}D$^+$–^{2}A$^-$ is suggested. A single exponential decay, as observed in the time resolved measurements, requires that the equilibrium is far on the side of ^{1}D*–A. Otherwise, it would be possible to monitor the equilibration of the system. Based on this assumption, a steady state approximation can employed for [^{2}D$^+$–^{2}A$^-$], and the decay of ^{1}D*–A can be expressed by ($k_{CR} = k_{CR}^G + k_{CR}^T$):

$$\frac{d[^1D^*\!-\!A]}{dt} = -\left(k_F + k_{IC} + k_{ISC} + \frac{k_{CS}k_{CR}}{k_{-CS} + k_{CR}} \right) \cdot [^1D^*\!-\!A] \qquad \text{Equ. 5}$$

The sum of k_F, k_{IC} and k_{ISC} is given the inverse fluorescence lifetime ($1/\tau_F^{ref}$) of the reference compound (**3**). If it is further supposed that $k_{-CS} >> k_{CR}$, Equ. 5 can be simplified to Equ. 6 with the equilibrium constant $K = k_{CS}/k_{-CS} = \exp(-\Delta G_{CS}^0 / RT)$:

$$\frac{d[^1D^*\!-\!A]}{dt} = -(1/\tau_F^{ref} + K \cdot k_{CR}) \cdot [^1D^*\!-\!A] = -\frac{1}{\tau_F(\varepsilon)} \cdot [^1D^*\!-\!A] \qquad \text{Equ. 6}$$

This latter approximation is possible in this case because ΔG_{-CS} is considered to be around 0 eV, resulting in electron transfer rates that are usually about 10^{10} s^{-1} [21], whereas k_{CR} is on the order of 10^8 s^{-1} (see below). Equ. 6 leads to the expectation of first order kinetics, as observed for (**4**), and allows the evaluation of the polarity dependence of the measured

fluorescence lifetimes $\tau_F(\varepsilon)$. Hereto, ΔG^0_{CS} was again obtained by Equ. 4, however with $R_{DA} = 7$ Å (including the approximate length of the methoxy linkers). The quantities k_{CR} and $\Delta G^0_{CS}(\mathrm{ACN})$ corresponding to $(E_{ox}(\mathrm{D})–E_{red}(\mathrm{A}))_{ACN}–E_{ex}$ in Equ. 4, were taken as free parameters. From the fit of the model function (solid line in Fig. 4) to the $\tau_F(\varepsilon)$ data, values of $k_{CR} = 3\times10^8$ s^{-1} and $\Delta G^0_{CS}(\mathrm{ACN}) = (+0.09 \pm 0.06)$ eV were obtained, which is in fact close to zero as expected from the electrochemical data. As Φ_{ISC} of (**4**) remains constant, despite the decrease of Φ_F, the CR reaction of $[^2D^+–{}^2A^-]$ leads most likely to considerable formation of the triplet state species $^3D^*–A$ with k^T_{CR} being on the order of 10^8 s^{-1}. It is illustrative to investigate the temperature dependence of the term $K\cdot k_{CR}$ in Equ. 6, which can be described using the Eyring equation for k_{CR}:

$$K \cdot k_{CR} = \exp(-\Delta G^0_{CS} / RT) \cdot k^0_{CR} \cdot \exp(-\Delta G^{\#}_{CR} / RT) = \\ = k^0_{CR} \cdot \exp(-(\Delta G^0_{CS} + \Delta G^{\#}_{CR}) / RT) \qquad \text{Equ. 7}$$

The temperature dependence of $K\cdot k_{CR}$ of (**4**), as obtained from $1/\tau_F$(**4**)–$1/\tau_F$(**3**) at each temperature in acetonitrile, is shown in Fig. 5. Obviously, a significant variation by almost one order of magnitude occurs within the temperature interval 80 – 300 K. The constant low-temperature value derives from slightly different lifetimes of (**3**) and (**4**) (e. g., 30 and 28 ns at 80 K). From a corresponding fit, a value of (+0.12 ± 0.02) eV is obtained for the sum $\Delta G^0_{CS} + \Delta G^{\#}_{CR}$. As expected, this number is larger than that for $\Delta G^0_{CS}(\mathrm{ACN})$ of +0.09 eV obtained above.

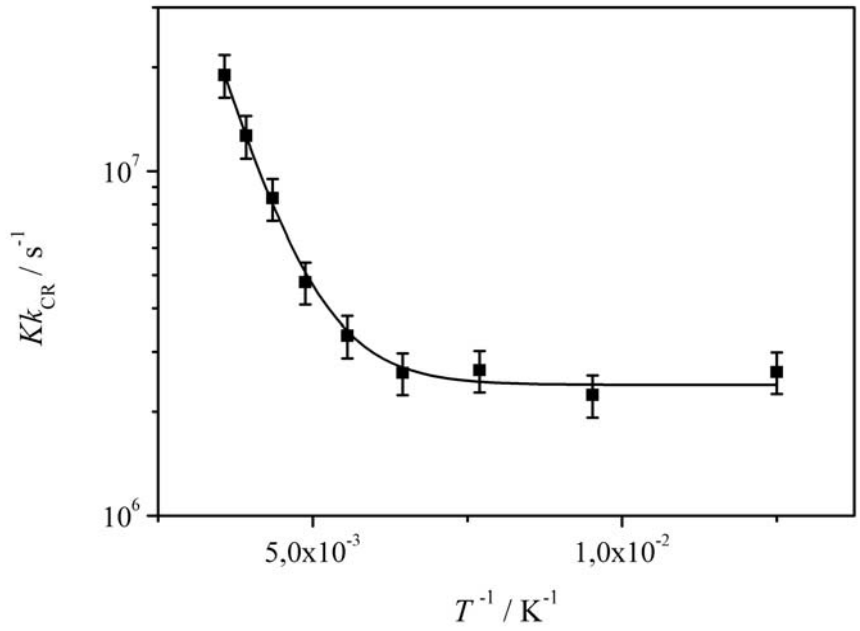

Fig. 5: Temperature dependence of $K \cdot k_{CR}$ in acetonitrile at 80–280 K. The solid line represents an exponential fit of the experimental data.

4. Conclusion

In this work, we demonstrate that electron transfer properties of angular [N]phenylenes, which may be of interest for functional donor-acceptor type dyads, can be described within the framework of the Marcus theory. The unsubstituted [N]phenylenes (**1**) and (**2**) exhibit a reorganization energy λ of 0.7 eV, which is smaller than the usual values for classical PAH (1.1 – 1.8 eV) [23]. As the internal reorganization energy λ is expected to be small for the [N]phenylene part, its value for the bimolecular electron transfer reactions is due mainly to the internal reorganization energy of the electron acceptor and the external reorganization energy.

The first electron transfer investigations of [N]phenylene bichromophors provide an interesting insight into intramolecular electron transfer reactions with positive ΔG^0_{CS} values, with special emphasis on the polarity tuning of the proposed equilibrium between the locally excited donor and the charge transfer complex. However, further work is required to identify and characterize the transient ionic species and to explore the possibility of practical use of angular [N]phenylene dyads. This is not possible with (**4**), because the percentage of the intramolecular charge transfer complex in the equilibrium is very small. Therefore, new [N]phenylene bichromophors are being targeted currently for synthesis, devoid of the perturbing carboxy groups attached to the [N]phenylene unit.

Acknowledgement

This work was funded by the Fonds der Chemischen Industrie, NSF (CHE-0451241) and the Deutscher Akademischer Austauschdienst (D/0103669). The Center for New Directions in Organic Synthesis is supported by Bristol-Myers Squibb as a Sponsoring Member and Novartis as a Supporting Member.

References

[1] For reviews of the phenylenes, see (a) O. Š. Miljanić and K. P. C. Vollhardt, in Carbon-Rich Compounds: Molecules to Materials, ed. M. M. Haley and R. R. Tykwinsky, Wiley-VCH, Weinheim, in press. (b) K. P. C. Vollhardt and D. L. Mohler, in Advances in Strain in Organic Chemistry, ed. B. Halton, JAI, London, 1996, pp 121–160.

[2] C. Dosche, H.-G. Löhmannsröben, A. Bieser, P. I. Dosa, S. Han, M. Iwamoto, A. Schleifenbaum and K. P. C. Vollhardt, Phys. Chem. Chem. Phys. 4 (2002) 2156.

[3] C. Dosche, M. U. Kumke, F. Ariese, A. N. Bader, C. Gooijer, P. I. Dosa, S. Han, O. S. Miljanic, K. P. C. Vollhardt, R. Puchta and N. J. R. van Eikema Hommes, Phys. Chem. Chem. Phys. 5 (2003) 4563.

[4] C. Dosche, M. U. Kumke, H.-G. Löhmannsröben, F. Ariese, A. N. Bader, C. Gooijer, O. S. Miljanic, M. Iwamoto, K. P. C. Vollhardt, R. Puchta and N. J. R. van Eikema Hommes, Phys. Chem. Chem. Phys. 6 (2004) 5476.

[5] N. J. Turro, Modern Molecular Photochemistry, University Science Books, Sausalito, 1991.

[6] S. Taillemite, C. Aubert, D. Fichou and M. Malacria, Tetr. Lett. 46 (2005) 8325.

[7] J.-F. Nierengarten, J.-F. Eckert, J.-F. Nicoud, L. Ouali, V. Krasnikov and G. Hadziioannou, Chem. Commun., 1999, 617.

[8] E. Peeters, P. A. van Hal, J. Knol, C. J. Brabec, N. S. Sariciftci, J. C. Hummelen, and R. A. J. Janssen, J. Phys. Chem. B, 104 (222)10174 .

[9] J. L. Segura, N. Martín and D. M. Guldi, Chem. Soc. Rev., 34 (2005) 31.

[10] J.-F. Nierengarten, New J. Chem., 28 (2004) 1177.

[11] R. Diercks and K. P. C. Vollhardt, Angew. Chem. 98 (1986) 268. Angew. Chem. Int. Ed. 25 (1986) 266.

[12] R. Diercks and K. P. C. Vollhardt, J. Am. Chem. Soc. 108 (1986) 3150.

[13] D. Holmes, S. Kumaraswamy, A. J. Matzger and K. P. C. Vollhardt, Chem. Eur. J. 5 (1999) 3399.

[14] S. L. Murov, I. Carmichael and G. L. Hug, Handbook of Photochemistry, 2nd edn., Marcel Dekker, New York, NY, 1993, 118.

[15] F. Lewitzka and H.-G. Löhmannsröben, Z. Phys. Chem. NF 150 (1986) 69.

[16] D. Rehm and A. Weller, Ber. Bunsenges. Phys. Chem. 73 (1969) 834.

[17] I. R. Gould and S. Farid, Acc. Chem. Res. 29 (1996) 522.

[18] H. G. O. Becker, Einführung in die Photochemie, 3rd edn., Deutscher Verlag der Wissenschaften, Berlin, 1991.

[19] A. Weller, Zeitschr. Phys. Chem. NF 133 (1982) 93.

[20] H. Heitele, P. Finckh, S. Weeren, F. Pöllinger and M. E. Michel-Beyerle, J. Phys. Chem. 93 (1989) 5173.

[21] T. Kakitani, A. Yoshimori and N. Mataga, J. Phys. Chem. 96 (1992) 5385.

[22] C. Burgdorff, H.-G. Löhmannsröben and T. Sander, J. Chem. Soc., Faraday Trans. 92 (1996) 3043.

[23] J. Balton, J. A. Schmidt, T.-F. Ho, J. Liu, K. J. Roach, A. C. Weedon, M. D. Archer, J. H. Wilford and V. P. Y. Gadzepko, Bridge Dependence of Photoinduced Intramolecular Electron Transfer, Electron Transfer in Inorganic, Organic and Biological Systems, Advances in Chemistry Series 228, Am. Chem. Soc., Washington, 1991.

[24] T. Kircher, Photoinduzierte Elektronentransferreaktionen eines Perylen-bis(carboximid)-Farbstoffes, Dissertation, Braunschweig, 1993.

[25] U. Wenzel and H.-G. Löhmannsröben, J. Photochem. Photobiol. A 96 (1996) 13.

[26] G. Lowe and D. D. Ridley, J. Chem. Soc. Chem. Commun. 1973, 328.

Synthetic section

Di(*para*-nitrobenzyl) acetylenedicarboxylate (5)

Acetylenedicarboxylic acid (2.00 g, 17.5 mmol), *para*-toluenesulfonic acid (203 mg, 1.18 mmol) and *para*-nitrobenzyl alcohol (6.83 g, 44.6 mmol) were diluted in toluene (40 ml). The solution was heated in a Dean-Stark apparatus (bath 145 ºC) until all the water had been removed. The resulting solution was washed with a saturated aqueous solution of $NaHCO_3$ (3 × 50 ml) and brine (50 ml). The toluene fraction was then dried over $MgSO_4$ and the solvent evaporated. The remaining solid was chromatographed over a silica gel column with 50% AcOEt/hexanes to yield the diester (**5**), 5.51 g (82%), as a white solid.

Mp = 106–107 ºC; UV-VIS (acetonitrile) λ_{max} (logε) = 223 (sh, 4.43), 266 (4.32) nm; MS (70 eV) *m/z* (rel. intensity) 384 (M^+, 17), 368 (16), 137 (100); ^{1}H NMR (300 MHz, $CDCl_3$) δ 8.25 (d, J = 8.8 Hz, 4H), 7.54 (d, J = 8.8 Hz, 4H), 5.36 (s, 4H); $^{13}C\{^1H\}$ NMR (300 MHz, $CDCl_3$) δ 151.0, 148.1, 140.8, 128.8, 123.9, 74.8, 66.9. Anal calcd for $C_{18}H_{12}O_8N_2$: C, 56.26; H, 3.15; N, 7.29. Found : C, 56.09; H, 3.40; N, 7.02. HRMS calcd for $C_{18}H_{12}O_8N_2$: 384.0594. Found : 384.0599.

Dibenzyl triangular [4]phenylene-2,3-dicarboxylate (**3**)

A solution of 5,6-bis(trimethylsilylethynyl) angular [3]phenylene (149 mg, 0.36 mmol) and Bu_4NF (1 ml of a 1.0 M solution in THF, 1.0 mmol) in degassed toluene (50 ml) was stirred at room temperature for 2 h. The reaction mixture was washed with degassed water (3 × 50 ml), dried over $MgSO_4$ and filtered into a 100 ml flask. To it was added $CpCo(CO)_2$ (100 μL, 0.78 mmol) and di(benzyl) acetylenedicarboxylate (2.31 g, 7.80 mmol),[26] and the mixture was transferred into a 50 ml syringe. The solution was injected into boiling toluene (100 ml) over a 10 h period. During the addition and for an additional 8 h, the reaction mixture was irradiated with a slide projector lamp. After cooling to room temperature, the toluene was removed under reduced pressure. The solid residue was purified by chromatography on silica gel with 2:1 AcOEt/hexanes to yield a crude product, which crystallized by adding hexanes to a diethyl ether solution to give a yellow solid. Kugelrohr distillation produced 13 mg (6.4 %) of (**3**) as a bright yellow solid.

Mp = 195–196 ºC; UV-VIS (acetonitrile) λ_{max} (logε) 227 (sh, 4.61), 243 (sh, 4.66), 248 (4.72), 257 (4.76), 287 (sh, 4.66), 297 (4.79), 308 (sh, 4.85), 313 (4.95), 317 (sh, 4.92), 333 (sh, 4.47), 340 (sh, 4.45), 351 (4.42), 362 (sh, 4.29), 377 (sh, 4.17), 397 (sh, 4.03), 425 (sh, 3.77), 460 (3.77) nm; MS (70 eV) *m/z* (rel. intensity) 568 (M^+, 100), 371 (31), 298 (43), 91 (100); ^{1}H NMR (400 MHz, $CDCl_3$) δ 7.47 (s, 2H), 7.32–7.39 (m, 10H), 7.19 (s, 8H), 5.22 (s, 4H); $^{13}C\{^1H\}$ NMR (300 MHz, $CDCl_3$) δ 167.3, 150.6, 148.7, 147.8, 135.4, 132.9, 132.4, 130.8, 129.4, 129.1, 128.6, 128.6, 128.4, 127.9, 120.3, 120.1, 119.5, 67.6. HRMS calcd for $C_{40}H_{24}O_4$: 568.1675. Found : 568.1662.

Di(*para*-nitrobenzyl) triangular [4]phenylene-2,3-dicarboxylate (4)

A solution of 5,6-bis(trimethylsilylethynyl) angular [3]phenylene (151 mg, 0.36 mmol) and Bu_4NF (1 ml of a 1.0 M solution in THF, 1.0 mmol) in degassed toluene (50 ml) was permitted to stir at room temperature for 2 h. The reaction mixture was washed with degassed water (3 × 50 ml), dried over $MgSO_4$, and filtered into a 100 ml flask. All these steps were

carried out in a glove bag flushed with N_2. To this mixture was added $CpCo(CO)_2$ (100 μL, 0.78 mmol), and the solution was transferred into a 50 ml syringe. The solution was injected into boiling toluene (100 ml) containing the diester (**5**) (3.09 g, 8.0 mmol) over an 11 h period. During the addition and for an additional 8 h, the reaction mixture was irradiated with a slide projector lamp. After cooling to room temperature, the toluene was removed under reduced pressure. The solid residue was purified by chromatography on silica gel with 50% AcOEt/hexanes to yield a crude red product, which was washed twice with AcOEt to provide 15.6 mg (6.6 %) of (**4**) as a yellow solid.

Mp = 234ºC; UV-VIS (acetonitrile) λ_{max} (logε) 239 (4.57), 248 (4.49), 261 (4.62), 271 (4.67), 277 (4.67), 287 (4.78), 301 (4.32), 307 (4.26), 313 (4.26), 319 (4.27), 326 (4.14), 332 (4.28), 341 (sh, 3.75), 355 (sh, 3.63), 361 (3.76), 460 (3.29) nm; MS (FAB) *m/z* 659 (MH^+); ^{1}H NMR (400 MHz, $CDCl_3$) δ 8.22 (d, J = 8.7 Hz, 4H), 7.55 (d, J = 8.7 Hz, 4H), 7.51 (s, 2H), 7.22 (m, 8H), 5.37 (s, 4H); $^{13}C\{^1H\}$ NMR (400 MHz, $CDCl_3$) δ 167.0, 151.1, 148.9, 147.8, 147.6, 142.5, 133.4, 131.7, 129.7, 129.2, 128.6, 127.6, 126.4, 123.9, 120.4, 120.2, 119.4, 77.9. Anal calcd for $C_{40}H_{22}O_8N_2$: C, 72.95; H, 3.37; N, 4.25. Found : C, 71.19; H, 3.80; N, 4.50.